Experimental Based Substructuring Using a Craig-Bampton Transmission Simulator Model

Mathew S. Allen,
Daniel C. Kammer
Department of Engineering Physics
University of Wisconsin
Madison, WI 53706
kammer@engr.wisc.edu, msallen@engr.wisc.edu
&
Randy L. Mayes
Structural Dynamics
Sandia National Laboratories[1]
Albuquerque, NM
rlmayes@sandia.gov

Keywords: experimental substructures, substructuring, Craig-Bampton

ABSTRACT

Recently, a new experimental based substructure formulation was introduced which reduces ill-conditioning due to experimental measurement noise by imposing the connection constraints on substructure modal coordinates instead of the physical interface coordinates. The experimental substructure is tested in a free-free configuration, and the interface is exercised by attaching a flexible transmission simulator. An analytical representation of the fixture is then used to subtract its effects from the experimental substructure. The resulting experimental component is entirely modal based, and can be attached in an indirect manner to other substructures by constraining the modal degrees of freedom of the transmission simulator to those substructures. This work explores a different alternative in which the transmission simulator is modeled with a Craig-Bampton model, a model that may be more appropriate when the interfaces are connected rigidly. The new method is compared to the authors' previous approaches to evaluate the errors due to modal truncation using finite element models of several beam systems including one in which the transmission simulator is connected to the component of interest at two points, potentially producing an ill-conditioned inverse problem.

1. Introduction

Experimental-analytical substructuring is attractive in many applications where there is motivation to replace one subcomponent with an experimental model. For example, a component may be difficult to model if it contains materials with unknown properties, intricate geometry that would require many elements to approximate or joints or interfaces with unknown stiffness and damping properties. In other cases the component may be produced by an external supplier, in which case it may be inefficient to expend effort modeling a component that one cannot change. In any case, it will be necessary to test the component at some point in order to validate the computational model. In these scenarios, one can perform a careful dynamic test and extract an experimental-based model for the subcomponent(s) of interest. This model can then be coupled to finite element (or other) models for the rest of the structure to predict the response.

Substructuring can be used to couple physical or modal models of each subcomponent to create a model (e.g. a set of ordinary differential equations) for the assembly, or, for linear systems, one can also operate on the frequency responses directly to predict those of the assembled system. The latter approach is called frequency based substructuring or impedance coupling and an excellent review is provided in [1]. This work focuses on the former, which is commonly referred to as

[1]Sandia National Laboratories is a multi-program laboratory managed and operated by Sandia Corporation, a wholly owned subsidiary of Lockheed Martin Corporation, for the U.S. Department of Energy National Nuclear Security Administration under Contract DE-AC04-94AL85000.

modal substructuring, although the authors have found that frequency based substructuring and modal substructuring give similar results when the data sets used are identical [2, 3].

In [4] Allen, Mayes & Bergman presented a specific substructuring strategy, now known as the Transmission Simulator (TS) method, in which the component of interest is tested with a fixture known as the transmission simulator attached in order to improve the experimental model for the component. The transmission simulator allows one to capture the compliance and damping of the bolted joints at the interface, provides a means for dealing with continuous, compliant interfaces where one cannot easily reduce the interface to a few connection points, and improves the modal basis of the experimental component by exercising the interface. The disadvantage to this approach is that the transmission simulator must be modeled very accurately and its model must be subtracted from the experimental model, potentially introducing negative mass or stiffness [5, 6].

In the authors' previous works, the transmission simulator has always been modeled with a free interface. More specifically, the modal model for the TS was described by up to six rigid body modes and a collection of elastic modes where all of the connection points were free. This basis may not be ideal in some applications, especially when the TS is rigidly connected to a stiff structure of interest. This work explores a new alternative where a Craig-Bampton model of the TS is created and substracted from the experimental measurements. Hence, the modal basis is described by the fixed-interface modes of the TS rather than its free modes, and this has been found to improve the results in a few test cases.

The following section reviews the theory underlying the transmission simulator method and how the transmission simulator model is replaced with a Craig-Bampton model. The method is evaluated on a T-shaped beam structure in Section 3 and conclusions are presented in Section 4.

2. Theoretical Development

2.1 Free-Free Modal Transmission Simulator (FF-TS)

The transmission simulator method is explained in detail in [4, 7, 8] so only a cursory review will be presented here. One is presumed to have a finite element model of the transmission simulator, denoted substructure A, and this can be used to compute its mode shapes, $\mathbf{\Phi}^{\mathrm{A}}$, natural frequencies, $\omega_r^{\mathrm{A}}, r = 1...n_{\mathrm{A}}$ and its modal damping ratios, ζ_r^{A} are also presumed to be known (e.g. they are typically taken to be half of the loss modulus of the material). In the traditional approach, these are computed with the interface degrees of freedom free, and hence the first few modes are rigid body modes. An actual physical transmission simulator is also constructed and attached to the substructure of interest, denoted B, and the assembly, denoted C, is tested to identify its modal parameters. The equations of motion of C and (–A) can then be concatenated as follows

$$\begin{bmatrix} \mathbf{I}^{\mathrm{C}} & 0 \\ 0 & -\mathbf{I}^{\mathrm{A}} \end{bmatrix} \begin{Bmatrix} \ddot{\mathbf{q}}^{\mathrm{C}} \\ \ddot{\mathbf{q}}^{\mathrm{A}} \end{Bmatrix} + \begin{bmatrix} \left[\backslash 2\zeta_r \omega_r \backslash \right]^{\mathrm{C}} & \mathbf{0} \\ \mathbf{0} & -\left[\backslash 2\zeta_r \omega_r \backslash \right]^{\mathrm{A}} \end{bmatrix} \begin{Bmatrix} \dot{\mathbf{q}}^{\mathrm{C}} \\ \dot{\mathbf{q}}^{\mathrm{A}} \end{Bmatrix} + \begin{bmatrix} \left[\backslash \omega_r^2 \backslash \right]^{\mathrm{C}} & \mathbf{0} \\ \mathbf{0} & -\left[\backslash \omega_r^2 \backslash \right]^{\mathrm{A}} \end{bmatrix} \begin{Bmatrix} \mathbf{q}^{\mathrm{C}} \\ \mathbf{q}^{\mathrm{A}} \end{Bmatrix} = \begin{Bmatrix} \left(\mathbf{\Phi}^{\mathrm{C}} \right)^{\mathrm{T}} \mathbf{F}^{\mathrm{C}} \\ \left(\mathbf{\Phi}^{\mathrm{A}} \right)^{\mathrm{T}} \mathbf{F}^{\mathrm{A}} \end{Bmatrix}$$
$$\begin{Bmatrix} \mathbf{u}^{\mathrm{C}} \\ \mathbf{u}^{\mathrm{A}} \end{Bmatrix} = \begin{bmatrix} \mathbf{\Phi}^{\mathrm{C}} & \mathbf{0} \\ \mathbf{0} & \mathbf{\Phi}^{\mathrm{A}} \end{bmatrix} \begin{Bmatrix} \mathbf{q}^{\mathrm{C}} \\ \mathbf{q}^{\mathrm{A}} \end{Bmatrix} \tag{1}$$

where the DOF, **q**, are the generalized modal coordinates of each substructure. Let the set of degrees of freedom where the TS joins the substructure be denoted as the c-set (or connection point set). Then one would ideally enforce equal motion between substructure C and the TS at these points.

$$\mathbf{u}_{\mathrm{c}}^{\mathrm{C}} = \mathbf{u}_{\mathrm{c}}^{\mathrm{A}} \tag{2}$$

However, this leads to several difficulties and hence Allen, Mayes & Bergman, instead defined a set of measurement points that completely characterize the transmission simulator (e.g. so that $\mathbf{\Phi}_m^{\mathrm{A}}$ is full rank). Then the following constraints are enforced, which constrain all of the modes of the transmission simulator to their projection onto the motion of C,

$$\begin{bmatrix} \left(\mathbf{\Phi}_m^{\mathrm{A}} \right)^{\dagger} \mathbf{\Phi}_m^{\mathrm{C}} & -\mathbf{I}^{\mathrm{A}} \end{bmatrix} \begin{Bmatrix} \mathbf{q}^{\mathrm{C}} \\ \mathbf{q}^{\mathrm{A}} \end{Bmatrix} = 0 \tag{3}$$

where, ()† , denotes the pseudo-inverse of the matrix (). These constraints are enforced using the transformation $\begin{bmatrix} \mathbf{q}_{\mathrm{C}}{}^{\mathrm{T}} & \mathbf{q}_{\mathrm{A}}{}^{\mathrm{T}} \end{bmatrix}^{\mathrm{T}} = \mathbf{B}\mathbf{q}_{\mathrm{C}}$ where $\mathbf{B} = \begin{bmatrix} \left(\mathbf{I}^{\mathrm{C}} \right)^{\mathrm{T}} & \left(\left(\mathbf{\Phi}_m^{\mathrm{A}} \right)^{\dagger} \mathbf{\Phi}_m^{\mathrm{C}} \right)^{\mathrm{T}} \end{bmatrix}^{\mathrm{T}}$ is in the null space of the constraint matrix, the matrix on the left in Eq. (3).

This method will only succeed in proportion to how well the modes of the transmission simulator, $\mathbf{\Phi}_m^{\mathrm{A}}$, span the space of the motions observed on C, or $\mathbf{\Phi}_m^{\mathrm{C}}$. While the free-interface modes have worked well in the cases studied so far, the authors have noted cases where these modes did not adequately span the space of the observed motions (see, e.g. [5]), leading to less accurate results or negative mass in the assembled system. Furthermore, it would be preferable to obtain a Craig-Bampton model for the subcomponent, with its constraint modes that capture the interface stiffness and allow it to accurately capture the motion of the subcomponent when it is connected to a variety of structures.

2.2 Craig-Bampton Transmission Simulator

In order to create a Craig-Bampton (CB) model of the transmission simulator, the physical displacement vector for substructure A is partitioned into two sets, the c-set, corresponding to the connection degrees of freedom, and the o-set, corresponding to the interior degrees of freedom (DOF). The resulting partitioned mass and stiffness matrices can be written as

$$\mathbf{M}^{\mathbf{A}} = \begin{bmatrix} \mathbf{M}_{\mathbf{oo}}^{\mathbf{A}} & \mathbf{M}_{\mathbf{oc}}^{\mathbf{A}} \\ \mathbf{M}_{\mathbf{co}}^{\mathbf{A}} & \mathbf{M}_{\mathbf{cc}}^{\mathbf{A}} \end{bmatrix} \qquad \mathbf{K}^{\mathbf{A}} = \begin{bmatrix} \mathbf{K}_{\mathbf{oo}}^{\mathbf{A}} & \mathbf{K}_{\mathbf{oc}}^{\mathbf{A}} \\ \mathbf{K}_{\mathbf{co}}^{\mathbf{A}} & \mathbf{K}_{\mathbf{cc}}^{\mathbf{A}} \end{bmatrix} \tag{4}$$

The displacement vector for component A can be transformed into CB [9] coordinates using the relation

$$\mathbf{u}^{\mathrm{A}} = \begin{Bmatrix} \mathbf{u}_o^{\mathrm{A}} \\ \mathbf{u}_c^{\mathrm{A}} \end{Bmatrix} = \begin{bmatrix} \hat{\mathbf{\Phi}}^{\mathrm{A}} & \boldsymbol{\psi}^{\mathrm{A}} \\ \mathbf{0} & \mathbf{I}_c \end{bmatrix} \begin{Bmatrix} \hat{\mathbf{q}}^{\mathrm{A}} \\ \mathbf{u}_c^{\mathrm{A}} \end{Bmatrix} = \mathbf{T}_{CB}^{\mathrm{A}} \mathbf{u}_{CB}^{\mathrm{A}} \tag{5}$$

where $\hat{\mathbf{\Phi}}^{\mathbf{A}}$ is a matrix of n_A fixed-interface modes, $\boldsymbol{\psi}^{\mathbf{A}} = -\left(\mathbf{K}_{\mathbf{oo}}^{\mathbf{A}}\right)^{-1} \mathbf{K}_{\mathbf{oc}}^{\mathbf{A}}$, $\mathbf{I_c}$ is an identity matrix of order equal to the number of interface DOF, $\hat{\mathbf{q}}^{\mathbf{A}}$ is the vector of displacements of the fixed-interface modes, and $\mathbf{u}_{\mathbf{c}}^{\mathbf{A}}$ represents the physical displacement of the interface. The CB representation describes the deformation of the transmission simulator in terms of dynamic fixed-interface modes, and static shapes, called constraint modes $\Psi^{\mathrm{A}} = \left[\left(\boldsymbol{\psi}^{\mathrm{A}}\right)^{\mathrm{T}} \quad \mathbf{I}_c\right]^{\mathrm{T}}$, in which each column gives the static response of component *A* due to a unit deflection of one of the interface DOF holding the others fixed. The corresponding CB mass and stiffness matrices are then given by

$$\mathbf{M}_{\mathbf{CB}}^{\mathbf{A}} = \left(\mathbf{T}_{\mathbf{CB}}^{\mathbf{A}}\right)^{\mathbf{T}} \mathbf{M}^{\mathbf{A}} \mathbf{T}_{\mathbf{CB}}^{\mathbf{A}} = \begin{bmatrix} \mathbf{I}^{\mathbf{A}} & \mathbf{M}_{\mathbf{qc}}^{\mathbf{A}} \\ \mathbf{M}_{\mathbf{cq}}^{\mathbf{A}} & \mathbf{M}_{\mathbf{S}}^{\mathbf{A}} \end{bmatrix} \tag{6}$$

$$\mathbf{K}_{\mathbf{CB}}^{\mathbf{A}} = \left(\mathbf{T}_{\mathbf{CB}}^{\mathbf{A}}\right)^{\mathbf{T}} \mathbf{K}^{\mathbf{A}} \mathbf{T}_{\mathbf{CB}}^{\mathbf{A}} = \begin{bmatrix} \left[\hat{\omega}_{\mathbf{r}}^2\right]^{\mathbf{A}} & 0 \\ 0 & \mathbf{K}_{\mathbf{S}}^{\mathbf{A}} \end{bmatrix} \tag{7}$$

where it has been assumed that the fixed-interface modes have been mass normalized, $\left[\hat{\omega}_{\mathbf{r}}^2\right]^{\mathbf{A}}$ is a diagonal matrix of fixed-interface modal frequencies, and $\mathbf{M}_{\mathbf{S}}^{\mathbf{A}}$ and $\mathbf{K}_{\mathbf{S}}^{\mathbf{A}}$ are the component A mass and stiffness matrices statically reduced to the interface DOF, respectively. As mentioned previously, the advantage of this transmission simulator representation over a free-free modal representation is that the fixed-interface modes do a better job of representing the shape of the simulator in the coupled system being tested, and the physical interface DOF are directly retained for connection to other substructures.

The CB representation of component A must now be subtracted from the experimental modal representation of the combined system C. The authors have explored two methods for doing this, which will be outlined in the following two subsections.

2.2.1 Method 1: Free Modes of Craig Bampton Model (CB-TS)

The CB representation of substructure A has the following equation of motion (omitting the damping terms for simplicity)

$$\mathbf{M}_{CB}^{\mathrm{A}} \ddot{\mathbf{u}}_{\mathrm{CB}}^{\mathrm{A}} + \mathbf{K}_{CB}^{\mathrm{A}} \mathbf{u}_{\mathrm{CB}}^{\mathrm{A}} = \left(\mathbf{T}_{CB}^{\mathrm{A}}\right)^{\mathrm{T}} \mathbf{F}^{\mathrm{A}} \tag{8}$$

This model can then replace the model for A in Eq. (1), so the concatenated equations become,

$$\begin{bmatrix} \mathbf{I}^{\mathrm{C}} & 0 \\ 0 & -\mathbf{M}^{\mathrm{A}}_{CB} \end{bmatrix} \begin{Bmatrix} \ddot{\mathbf{q}}^{\mathrm{C}} \\ \ddot{\mathbf{u}}^{\mathrm{A}}_{\mathrm{CB}} \end{Bmatrix} + \begin{bmatrix} \left[\backslash \omega_r^{\,2} \backslash \right]^{\mathrm{C}} & \mathbf{0} \\ \mathbf{0} & -\mathbf{K}^{\mathrm{A}}_{CB} \end{bmatrix} \begin{Bmatrix} \mathbf{q}^{\mathrm{C}} \\ \mathbf{u}^{\mathrm{A}}_{\mathrm{CB}} \end{Bmatrix} = \begin{Bmatrix} \left(\mathbf{\Phi}^{\mathrm{C}}\right)^{\mathrm{T}} \mathbf{F}^{\mathrm{C}} \\ \left(\mathbf{T}^{\mathrm{A}}_{CB}\right)^{\mathrm{T}} \mathbf{F}^{\mathrm{A}} \end{Bmatrix}$$
$$\begin{Bmatrix} \mathbf{u}^{\mathrm{C}} \\ \mathbf{u}^{\mathrm{A}} \end{Bmatrix} = \begin{bmatrix} \mathbf{\Phi}^{\mathrm{C}} & \mathbf{0} \\ \mathbf{0} & \mathbf{T}^{\mathrm{A}}_{CB} \end{bmatrix} \begin{Bmatrix} \mathbf{q}^{\mathrm{C}} \\ \mathbf{u}^{\mathrm{A}}_{\mathrm{CB}} \end{Bmatrix} \tag{9}$$

In keeping with the modal constraint philosophy, all of the modes of the transmission simulator will be coupled to their projection on C, using the following constraints, where once again the measurement set, *m*, includes enough sensors to fully characterize the motion of the transmission simulator.

$$\begin{bmatrix} \left(\mathbf{T}^{\mathrm{A}}_{\mathrm{CB},m}\right)^{\dagger} \mathbf{\Phi}^{\mathrm{C}}_{m} & -\mathbf{I}^{\mathrm{A}} \end{bmatrix} \begin{Bmatrix} \mathbf{q}^{\mathrm{C}} \\ \mathbf{u}^{\mathrm{A}}_{\mathrm{CB}} \end{Bmatrix} = 0 \tag{10}$$

Since the model for substructure A is known, after assembling the system one can recover the response at any point on A (including the connection point $\mathbf{u}^{\mathrm{A}}_{\mathrm{c}}$, both displacement and rotation!) using Eq. (5). Hence, one can estimate the fixed-interface modes of the B system by applying the constraints $\mathbf{u}^{\mathrm{A}}_{\mathrm{c}} = 0$ by defining an appropriate transformation matrix, **B**, and then using the procedure outlined above. It is also interesting to note that one could obtain the same result by using the CB model to estimate the free-interface modes of the TS and then using those in Eq. (1) together with the usual transmission simulator approach. The free-interface modes thus estimated would not be the true free-interface modes but simply another basis for the CB model, and hence this would produce the exact same result as the procedure outlined in Eqs. (9) and (10). In fact, this approach was used in this computations described in Section 3.

2.2.2 Method 2: Motion Relative to the Interface (CB-IP)

The method presented in the previous section is clearly very different from the way in which Craig Bampton models have been employed in the analytical domain over the past several decades. Specifically, no effort was made to retain the structure of the CB model nor the partition of interface degrees of freedom as unique coordinates. Hence, an alternative is presented here, which will be denoted CB-IP for "Interface Preserving."

Once again, following the modal constraint approach [4], coupling will be accomplished by enforcing physical displacement compatibility between the two components at the measured locations

$$\mathbf{u}^{\mathbf{A}}_{\mathbf{m}} - \mathbf{u}^{\mathbf{C}}_{\mathbf{m}} = 0 \tag{11}$$

where it is assumed that none of the connection DOF are in the set of measured locations. Transforming to CB coordinates for component A and modal coordinates for experimental component *C*, Eq. (11) becomes

$$\hat{\Phi}^{\mathbf{A}}_{\mathbf{m}} \hat{\mathbf{q}}^{\mathbf{A}} + \psi^{\mathbf{A}}_{\mathbf{m}} \mathbf{u}^{\mathbf{A}}_{\mathbf{c}} - \Phi^{\mathbf{C}}_{\mathbf{m}} \mathbf{q}^{\mathbf{C}} = 0 \tag{12}$$

in which the subscript m indicates a row partition corresponding to the measured DOF. Equation (12) can be solved for the transmission simulator fixed-interface modal response

$$\hat{\mathbf{q}}^{\mathbf{A}} = \hat{\Phi}^{\mathbf{A}\dagger}_{\mathbf{m}} \left[\Phi^{\mathbf{C}}_{\mathbf{m}} \mathbf{q}^{\mathbf{C}} - \psi^{\mathbf{A}}_{\mathbf{m}} \mathbf{u}^{\mathbf{A}}_{\mathbf{c}} \right] \tag{13}$$

where $\hat{\Phi}^{\mathbf{A}\dagger}_{\mathbf{m}} = \left[\hat{\Phi}^{\mathbf{AT}}_{\mathbf{m}} \hat{\Phi}^{\mathbf{A}}_{\mathbf{m}} \right]^{-1} \hat{\Phi}^{\mathbf{AT}}_{\mathbf{m}}$ is the generalized inverse of the fixed-interface modes row partitioned to the measurement locations. The existence of this inverse requires that matrix $\hat{\Phi}^{\mathbf{A}}_{\mathbf{m}}$ is full column rank, implying that $n_m \geq n_A$. Notice that the constraints here can be viewed as projecting the motion of C relative to the interface onto the fixed-interface modes of A.

The modal constraint can be applied by defining the coordinate transformation

$$\mathbf{u}_{\mathbf{G}} = \begin{Bmatrix} \mathbf{q}^{\mathbf{C}} \\ \hat{\mathbf{q}}^{\mathbf{A}} \\ \mathbf{u}^{\mathbf{A}}_{\mathbf{c}} \end{Bmatrix} = \mathbf{T}\mathbf{u}_{\mathbf{r}} = \begin{bmatrix} \mathbf{I} & 0 \\ \hat{\Phi}^{\mathbf{A}\dagger}_{\mathbf{m}} \Phi^{\mathbf{C}}_{\mathbf{m}} & -\hat{\Phi}^{\mathbf{A}\dagger}_{\mathbf{m}} \psi^{\mathbf{A}}_{\mathbf{m}} \\ 0 & \mathbf{I} \end{bmatrix} \begin{Bmatrix} \mathbf{q}^{\mathbf{C}} \\ \mathbf{u}^{\mathbf{A}}_{\mathbf{c}} \end{Bmatrix} \tag{14}$$

Applying the constraint to the uncoupled system in Eq. (9) gives the approximation of the equation of motion for the experimental based substructure B

$$\tilde{\mathbf{M}}^{\mathbf{B}}\ddot{\tilde{\mathbf{u}}}^{\mathbf{B}} + \tilde{\mathbf{K}}^{\mathbf{B}}\tilde{\mathbf{u}}^{\mathbf{B}} = \mathbf{T}^{\mathbf{T}}\begin{Bmatrix} \left(\Phi^{\mathbf{C}}\right)^{\mathbf{T}}\mathbf{F}^{\mathbf{C}} \\ \left(\mathbf{T}^{\mathbf{A}}_{\mathbf{CB}}\right)^{\mathbf{T}}\mathbf{F}^{\mathbf{A}} \end{Bmatrix} \tag{15}$$

in which the reduced displacement vector $\mathbf{u}_\mathbf{r}$ in Eq. (14) has been renamed $\tilde{\mathbf{u}}^{\mathbf{B}}$ where

$$\tilde{\mathbf{u}}^{\mathbf{B}} = \begin{Bmatrix} \tilde{\mathbf{q}}^{\mathbf{B}} \\ \tilde{\mathbf{u}}^{\mathbf{B}}_{\mathbf{c}} \end{Bmatrix} \tag{16}$$

and

$$\tilde{\mathbf{M}}^{\mathbf{B}} = \mathbf{T}^{\mathbf{T}}\begin{bmatrix} \mathbf{I}^{\mathbf{C}} & 0 \\ 0 & -\mathbf{M}^{\mathbf{A}}_{\mathbf{CB}} \end{bmatrix}\mathbf{T} = \begin{bmatrix} \mathbf{I}^{\mathbf{C}} - \boldsymbol{\tau}^{\mathbf{T}}\boldsymbol{\tau} & \boldsymbol{\tau}^{\mathbf{T}}\boldsymbol{\psi} - \boldsymbol{\tau}^{\mathbf{T}}\mathbf{M}^{\mathbf{A}}_{\mathbf{qc}} \\ \boldsymbol{\psi}^{\mathbf{T}}\boldsymbol{\tau} - \mathbf{M}^{\mathbf{A}}_{\mathbf{cq}}\boldsymbol{\tau} & \mathbf{M}^{\mathbf{A}}_{\mathbf{cq}}\boldsymbol{\psi} + \boldsymbol{\psi}^{\mathbf{T}}\mathbf{M}^{\mathbf{A}}_{\mathbf{qc}} - \boldsymbol{\psi}^{\mathbf{T}}\boldsymbol{\psi} - \mathbf{M}^{\mathbf{A}}_{\mathbf{S}} \end{bmatrix} \tag{17}$$

$$\tilde{\mathbf{K}}^{\mathbf{B}} = \mathbf{T}^{\mathbf{T}}\begin{bmatrix} \left[\backslash\hat{\boldsymbol{\omega}}^2_{\mathbf{r}\backslash}\right]^{\mathbf{C}} & 0 \\ 0 & -\mathbf{K}^{\mathbf{A}}_{\mathbf{CB}} \end{bmatrix}\mathbf{T} = \begin{bmatrix} \left[\backslash\hat{\boldsymbol{\omega}}^2_{\mathbf{r}\backslash}\right]^{\mathbf{C}} - \boldsymbol{\tau}^{\mathbf{T}}\left[\backslash\hat{\boldsymbol{\omega}}^2_{\mathbf{r}\backslash}\right]^{\mathbf{A}}\boldsymbol{\tau} & \boldsymbol{\tau}^{\mathbf{T}}\left[\backslash\hat{\boldsymbol{\omega}}^2_{\mathbf{r}\backslash}\right]^{\mathbf{A}}\boldsymbol{\psi} \\ \boldsymbol{\psi}^{\mathbf{T}}\left[\backslash\hat{\boldsymbol{\omega}}^2_{\mathbf{r}\backslash}\right]^{\mathbf{A}}\boldsymbol{\tau} & -\boldsymbol{\psi}^{\mathbf{T}}\left[\backslash\hat{\boldsymbol{\omega}}^2_{\mathbf{r}\backslash}\right]^{\mathbf{A}}\boldsymbol{\psi} - \mathbf{K}^{\mathbf{A}}_{\mathbf{S}} \end{bmatrix} \tag{18}$$

with $\boldsymbol{\tau} = \hat{\boldsymbol{\Phi}}^{\mathbf{A}\dagger}_{\mathbf{m}}\boldsymbol{\Phi}^{\mathbf{C}}_{\mathbf{m}}$ and $\boldsymbol{\psi} = \hat{\boldsymbol{\Phi}}^{\mathbf{A}\dagger}_{\mathbf{m}}\boldsymbol{\psi}^{\mathbf{A}}_{\mathbf{m}}$. The substructure representation for component B, given by Eqs. (17) and (18), is not precisely a CB representation because the stiffness matrix is not block diagonal. However, it is CB-like in that the displacement vector $\tilde{\mathbf{u}}^{\mathbf{B}}$ contains modal degrees of freedom $\tilde{\mathbf{q}}^{\mathbf{B}}$, and the physical degrees of freedom $\tilde{\mathbf{u}}^{\mathbf{B}}_{\mathbf{c}}$ at the points where component B will connect to other substructures. The experimental based representation for component B can then be easily connected to other FEM based substructures using traditional assembly methods. However, unlike the CB representation, the modal degrees of freedom cannot be truncated based on frequency due to the stiffness coupling between the modal and interface DOF in Eq. (18).

An advantage of the proposed component B substructure representation is that the fixed-interface modes and frequencies can be determined directly by just crossing out the block row and column associated with the interface DOF. The resulting constrained interface mass and stiffness matrices, $\tilde{\mathbf{M}}^{\mathbf{B}}_{\mathbf{c}}$ and $\tilde{\mathbf{K}}^{\mathbf{B}}_{\mathbf{c}}$, just correspond to the expressions in the upper-left quadrants of the matrices in Eqs. (17) and (18). Therefore, the fixed-interface modes and frequencies of component B can be derived from a free-free vibration test of the composite system C including the transmission simulator. If the proper number of free-free experimental modes for component C and fixed-interface modes from the transmission simulator are retained in the analysis, the matrices $\tilde{\mathbf{M}}^{\mathbf{B}}_{\mathbf{c}}$ and $\tilde{\mathbf{K}}^{\mathbf{B}}_{\mathbf{c}}$ should both be positive definite. Further details regarding this approach can be found in [10].

3. Numerical Examples

This new approach was explored by applying it to two systems, one of which was studied in a previous work [10]. The second system contains two connection points (statically indeterminate interface) and was developed specifically for this work.

3.1 T-Beam System from [10]

The first system studied is the T-beam system shown in Figure 1, which was used in [10] to demonstrate the method that will be denoted the CB-IP method here. The transmission simulator is a 24-in long steel beam with 0.5 by 0.5-in cross section while the structure of interest, component B, is a 36-in long steel beam with 0.35 by 0.5-in cross section. Note that this system's TS is significantly more flexible than that used in [4-6], so it is more difficult to subtract from the assembly. Further details regarding the setup are provided in [10]. As in the cited works, finite element models for these beams will be used to simulate substructuring by truncating the modal basis.

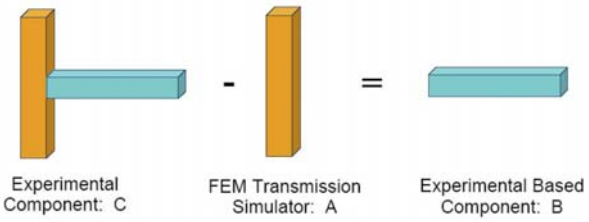

Figure 1: Schematic of the T-beam substructuring problem. The goal is to experimentally derive a model of component B, the horizontal (cyan) beam, from measurements of the assembly C.

As in [10], the frequency range of interest is 0 to 2500 Hz, so 24 modes of C are retained with natural frequencies ranging from 0 Hz (3 rigid body modes) to 4780 Hz, or over about twice the frequency range of interest. In [10], 13 fixed-interface modes were used to describe substructure A, with the highest mode at 15.9 kHz, and after applying 13 constraints a model for B was obtained. As a first step in evaluating the success of the substructuring calculations, the free modes of component B were calculated, and they are compared to those of the FEA truth model in Table 1 in the column labeled CB-IP.

The same process was repeated using the traditional transmission simulator method with free-interfaces modes, the FF-TS method, and the result of that calculation is compared with the proposed method which uses a Craig-Bampton model to describe the transmission simulator, the CB-TS method, and those results are also shown in Table 1. Both of these models used 10 modes to describe the transmission simulator, 3 rigid body modes plus 7 free-interface elastic modes for the FF-TS method and 3 constraint modes plus 7 fixed-interface modes for the CB-TS method. These modes spanned a frequency range of 0 to 13.7 kHz for the FF-TS method and 0 to 8.4 kHz for the CB-TS method. Note that because the interface (connection point) is at the center of the transmission simulator, its fixed interface modes came in pairs in which either the top or bottom vibrated as a cantilever while other side remained stationary. As a result, a larger number of modes would be required to span the same frequency range.

Table 1: Free-Interface Modes of component B estimated by each substructuring approach.

	Actual	CB-IP (Craig Bampton)		FF-TS (Free-Interface)			CB-TS (Craig Bampton)		
N	**FEA**	**Freq (Hz)**	**% Error**	**N**	**Freq (Hz)**	**% Error**	**N**	**Freq (Hz)**	**% Error**
4	45.4	45.4	**0.01%**	4	45.4	**0.00%**	4	45.4	**0.00%**
5	125.1	125.1	**0.00%**	5	125.1	**0.00%**	5	125.1	**0.00%**
6	245.3	245.4	**0.02%**	6	245.3	**0.00%**	6	245.3	**0.00%**
7	405.5	405.7	**0.05%**	7	405.5	**0.00%**	7	405.6	**0.01%**
8	605.8	606.5	**0.12%**	8	605.8	**0.01%**	8	606.0	**0.03%**
9	846.1	848.1	**0.23%**	9	846.2	**0.01%**	9	846.6	**0.05%**
10	1126.5	1131.2	**0.42%**	10	1126.8	**0.02%**	10	1127.5	**0.09%**
11	1447.0	1457.5	**0.72%**	11	1447.5	**0.04%**	11	1449.0	**0.14%**
12	1807.6	1829.6	**1.22%**	**13***	1808.6	**0.05%**	12	1811.3	**0.20%**
13	2118.7	2118.4	**-0.01%**	14	2118.8	**0.00%**	13	2128.9	**0.48%**
14	2208.3	2253.5	**2.05%**	15	2210.1	**0.08%**	14	2214.8	**0.30%**
15	2649.2	2741.3	**3.48%**	16	2652.3	**0.12%**	15	2660.3	**0.42%**
16	3130.3			**18***	3135.4	**0.16%**	**17***	3148.8	**0.59%**
17	3651.7			19	3659.8	**0.22%**	18	3682.1	**0.83%**
18	4213.6			20	4226.1	**0.30%**	19	4265.3	**1.23%**
19	4237.3			21	4237.4	**0.00%**	20	4480.4	**5.74%**
20	4816.0			22	4836.4	**0.42%**	21	4929.8	**2.36%**

**Spurious modes were omitted from the table.*

The results show that, while any of the methods produces good estimate of the B system's free-free natural frequencies in the frequency range of interest, the traditional FF-TS method is somewhat more accurate than the others. This is, perhaps, to be expected since our goal is to obtain a Craig-Bampton-like model for system B, and while a Craig-Bampton model would be excellent at describing B in an assembly, it might not produce the best results when the interface is free or lightly coupled. In those cases another subcomponent model, such as a Craig-Chang model [11], would probably be preferred and the FF-TS method produces a model that is more along those lines. On the other hand, the table also shows the mode number of each

mode that is being compared in the column labeled "N." The modes were matched using a MAC and so only modes that were similar are compared in the table. The FF-TS and CB-TS methods both show gaps in the mode number. The modes that are not shown had purely imaginary natural frequencies and hence were not included. The one exception was mode 12 in the FF-TS method which appeared to be reasonable. The gaps reveal that the first spurious mode occurred above 1400 Hz (after the 11th mode) for the FF-TS method and not until above 2660 Hz (after the 15th mode) for the CB-TS method. This could suggest that the CB-TS method captures the deformation of the transmission simulator more effectively.

When the component of interest will be connected to a fairly rigid substructure, it may be more important for the substructure model to accurately predict the component's fixed-interface modes rather than its free modes. The fixed-interface modes of each of the substructure models were derived by constraining the three interface DOF as mentioned in Sections 2.2.1 and 2.2.2. Then the fixed-interface natural frequencies were found and are compared in Table 2.

Table 2: Fixed-Interface Modes of component B estimated by each substructuring approach.

	Actual	CB-IP (Craig Bampton)			FF-TS (Free-Interface)			CB-TS (Craig Bampton)		
N	FEA	N	Freq (Hz)	% Error	N	Freq (Hz)	% Error	N	Freq (Hz)	% Error
1	7.127	1	7.14	**0.18%**	1	7.07	**-0.80%**	1	7.127	**0.00%**
2	44.707	2	44.71	**0.01%**	2	44.36	**-0.78%**	2	44.707	**0.00%**
3	125.19	3	125.2	**0.00%**	3	124.2	**-0.77%**	3	125.18	**0.00%**
4	245.32	4	245.3	**0.00%**	4	243.45	**-0.76%**	4	245.30	**-0.01%**
5	405.53	5	405.5	**0.00%**	5	402.48	**-0.75%**	5	405.49	**-0.01%**
6	605.80	6	605.8	**0.00%**	6	601.30	**-0.74%**	6	605.71	**-0.01%**
7	846.12	7	846.2	**0.01%**	7	839.91	**-0.74%**	7	845.95	**-0.02%**
8	1059.3	8	1059.3	**0.00%**	8	808.03	**-23.72%**	8	1059.3	**0.00%**
9	1126.5	9	1126.6	**0.01%**	9	1118.3	**-0.73%**	9	1126.2	**-0.03%**
10	1447.0	10	1447.1	**0.01%**	10	1436.5	**-0.72%**	10	1446.5	**-0.04%**
11	1807.6	11	1807.8	**0.01%**	11	1794.6	**-0.72%**	11	1806.8	**-0.04%**
12	2208.3	12	2208.6	**0.01%**	**13***	2192.6	**-0.71%**	12	2207.1	**-0.06%**
13	2649.2	13	2649.5	**0.01%**	14	2630.4	**-0.71%**	13	2647.4	**-0.07%**
14	3130.3	**16***	3130.7	**0.01%**	**16***	3108.3	**-0.70%**	**15***	3127.8	**-0.08%**
15	3178.0	17	3178.0	**0.00%**	17	3672.1	**15.55%**	16	3178.1	**0.00%**
16	3651.7	18	3652.3	**0.01%**	18	3626.2	**-0.70%**	17	3648.2	**-0.10%**
17	4213.6	19	4214.2	**0.01%**	19	4184.3	**-0.70%**	18	4208.6	**-0.12%**
18	4816.0	20	4815.5	**-0.01%**	20	4782.5	**-0.69%**	19	4809.4	**-0.14%**
19	5296.6	21	5327.3	**0.58%**	-	-	-	20	6289.3	**18.74%**
20	5459.2	22	5498.4	**0.72%**	-	-	-			
21	6143.3				21	6915.0	**26.67%**			

The results in Table 2 show that the methods that use a Craig Bampton basis to describe the transmission simulator produced considerably more accurate predictions of the fixed-interface modes. Indeed, both the CB-IP and CB-TS methods estimated all of the natural frequencies below 5 kHz (twice the bandwidth of interest) with less than 0.2% error. The errors for the CB-IP method are somewhat lower, although any of these modal truncation errors would probably be negligible relative to measurement errors when the methods are applied in practice. In contrast, while the natural frequencies predicted by the FF-TS method are quite reasonable for most of the modes (typically below 1%), the errors in modes 8 and 17 were quite large and the model contains a larger number of spurious modes. To diagnose this, the number of modes used to describe the TS in the FF-TS method was varied between 3 and 11. In all cases the FF-TS method predicted a reasonable number of free-interface modes correctly (e.g. with errors in the natural frequencies below 1%). It also gave reasonable estimates for the lower fixed-interface modes, with about 2% maximum error over the first eight modes for n_A=3 decreasing to less than 9% maximum error (1.5% average error) for the first 15 modes for n_A=8. As more modes were added to the TS modes 8 and 17 began to degrade as seen above while the other natural frequencies became even more accurate. In contrast, the CB-TS method gave excellent predictions for the fixed-interface modes for n_A>5, with all of the lower natural frequencies having less than 1% errors.

These results are somewhat surprising. While one would expect that, if one could create a Craig Bampton model for subcomponent B, that it would do an excellent job of predicting the fixed interface modes (actually the result would be perfect since the CB model contains the fixed-interface modes). However, here we have used a relatively small number of the free modes of the assembly C and a CB model for A to derive an approximate CB model for B by computing B=(C-A), and the result is excellent!

As has been mentioned in the authors' previous works [5, 6], when one substructure is subtracted from another it is possible for the mass matrix to become indefinite (contain negative eigenvalues), and these in turn tend to produce additional spurious modes in the substructuring predictions. The authors presented two algorithms in [6] to address this issue. The Craig-Bampton method presented in this work is essentially interchangeable with the FF-TS method in the authors previous works, so the same algorithms can be used to force positive mass when substructuring. This was explored here by using the "Added Mass" method in [6] to add mass to the substructure model for B until its mass matrix became positive definite. This algorithm was used to correct the models for B for the case presented in Tables 1 and 2 by adding the minimum amount of mass which caused the mass matrix to become positive definite. For the FF-TS method the mass added was 0.65% of the total mass of substructure B, while for the CB-TS method only 0.00015% mass had to be added. The added mass didn't change the CB-TS results appreciably. On the other hand, for the FF-TS method it was surprising to see that the added mass dramatically improved the predictions of 8^{th} and 17^{th} fixed interface modes, reducing the errors in those natural frequencies just a few percent. All of these results suggest that a Craig-Bampton model is a more accurate basis for the transmission simulator in this application.

In the authors previous works [4-6], they have also studied a T-beam system which is similar to that described here (and in [10]) although it had a stiffer transmission simulator. The CB-TS method was also applied to that system and the results obtained showed similar trends to those presented above, so for brevity those results will not be included here.

3.2 Two-dimensional Structure with Indeterminate Interface

In this next case study, a system is considered which could lead to an ill-conditioned substructuring problem. The system of interest is the C-shaped assembly highlighted with a dash-dot (blue) box in Figure 2. In the assembly of interest (on the left in Figure 2), system B is connected to another C-shaped beam creating a box structure with an additional appendage that is 305mm long. As shown in Figure 2, the beams that complete the box in the assembly of interest are thicker than those in B, having a height of 25mm where the beams comprising B have a height of 19mm. The box in both C and in the assembly of interest is 457 mm square and all of the beams had a width of 25mm. A transmission simulator was designed to replicate the C-shaped beam in the assembly of interest, although the cross section of the transmission simulator was 19mm high by 25mm thick, so it is less stiff than the system in the assembly of interest. All of the other dimensions were identical to those in the assembly of interest. The interface between the TS and system B consists of two separate arms and hence is reminiscent of the system studied by P. Ind in his PhD thesis [12]. Ind's work showed that a system such as this can exhibit dramatic sensitivity to noise because the measurements are likely to contain very little relative motion of the arms and yet that motion provides the only available information about how the structure will move once the transmission simulator is removed. However, in this case the problem should not be as poorly conditioned as the system studied by Ind because the transmission simulator does allow some motion of the interface DOF in its lower modes of vibration.

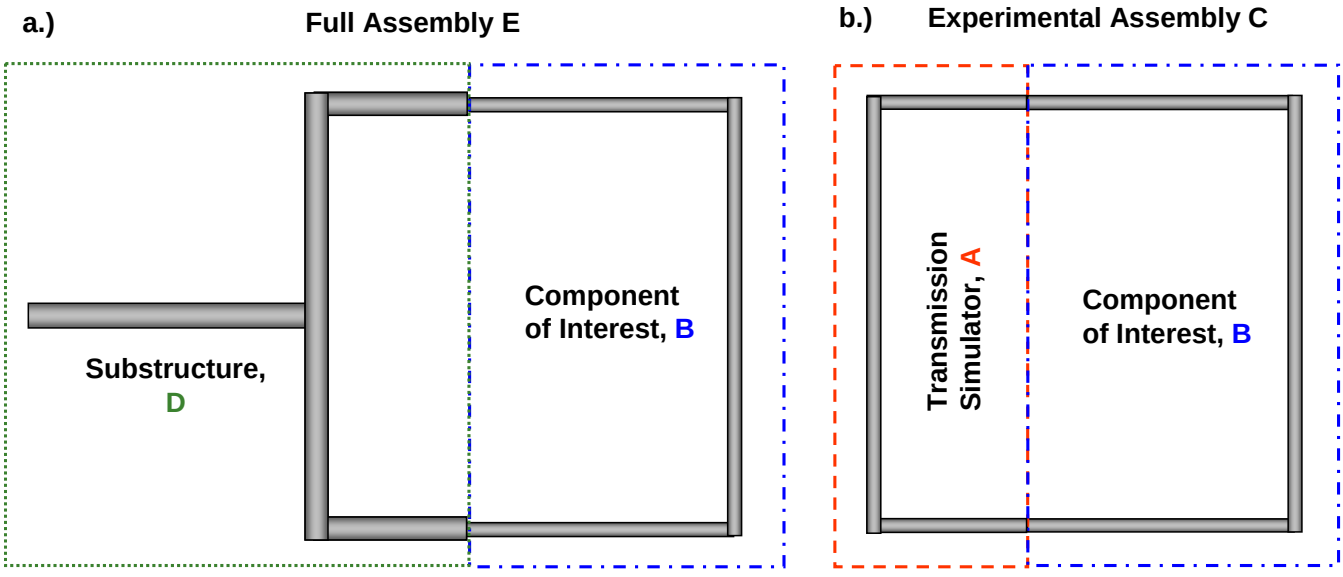

Figure 2: Schematic of two-dimensional structure with a statically indeterminate interface. a.) Full Assembly E=B+D, b.) Assembly C. We desire to predict the motion of the assembly on the left but wish to avoid creating an FEA model for B. A transmission simulator, A, is created and attached to B and the modes of the assembly are found and used to derive the model for B.

One dimensional FEA models were created for each beam, with 25 mm long elements, and the resulting nodes are shown in Figure 3. Duplicate nodes were merged when assembling the system. Then, to simulate a modal test the modes of the FEA model for assembly C were computed out to 3kHz, resulting in a 16 mode model for C that included three rigid body modes. A Craig Bampton model was then created of the transmission simulator, with six constraint modes and two elastic (fixed-interface) modes. Those two elastic modes were the only fixed-interface modes below 1kHz.

Figure 4 shows twelve of the thirteen elastic modes of Assembly C. (The first elastic mode, which is not shown, was a first ovaling mode along the diagonal of the frame.) The higher modes show considerable bending of the frame suggesting that a modal model based on these modes should be able to capture relatively complicated motion of component B. The fixed interface and constraint modes of the transmission simulator are shown in Figures 5 and 6 respectively. This truncated model for the TS was evaluated by computing its free-interface modes and comparing their natural frequencies with the true free-interface natural frequencies. This revealed that the Craig-Bampton model for the TS accurately predicted the first three modes of the free-free transmission simulator (up to 650 Hz) to within 1.2%, while the next few modes (beginning at 1.2 kHz) were not predicted accurately, although their shapes were vaguely similar.

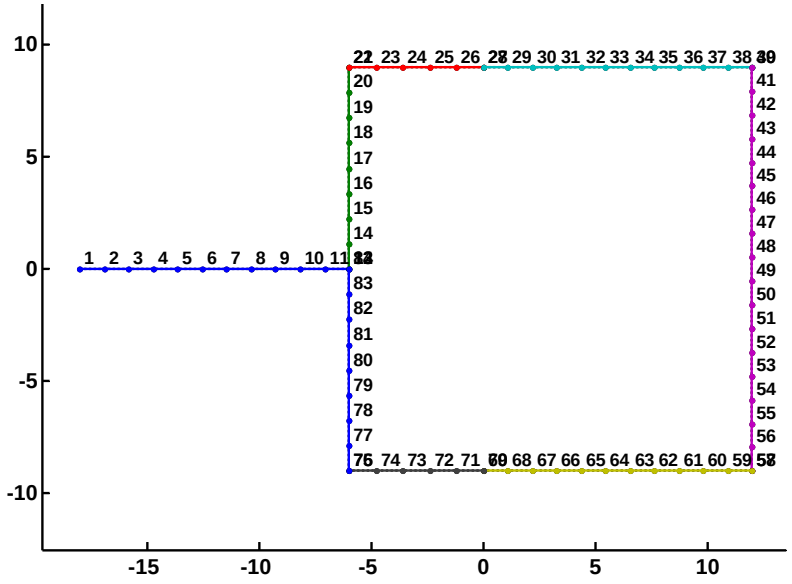

Figure 3: Finite Element Mesh of the Assembly of Interest.

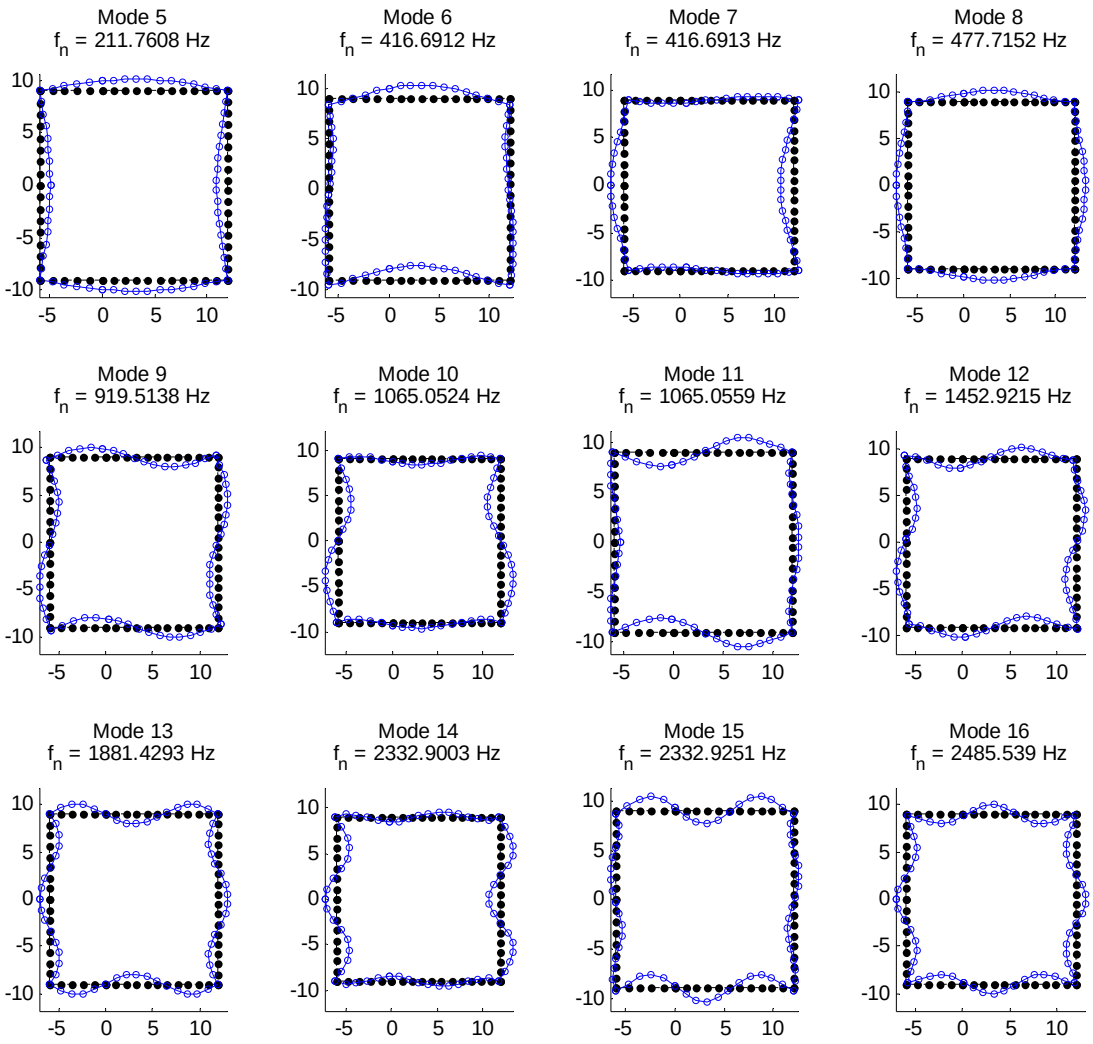

Figure 4: Elastic modes of Assembly C in the frequency range of interest.

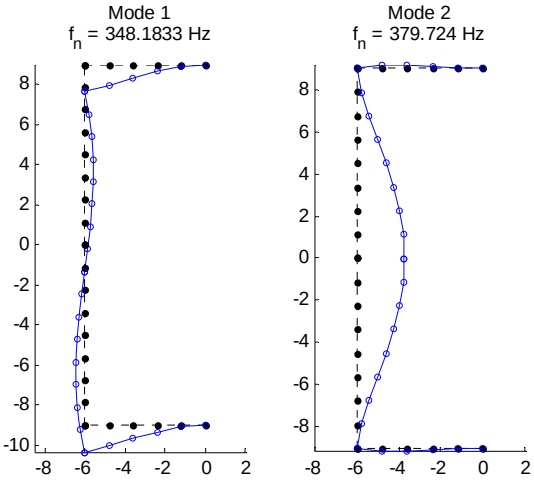

Figure 5: Fixed-interface modes of the transmission simulator.

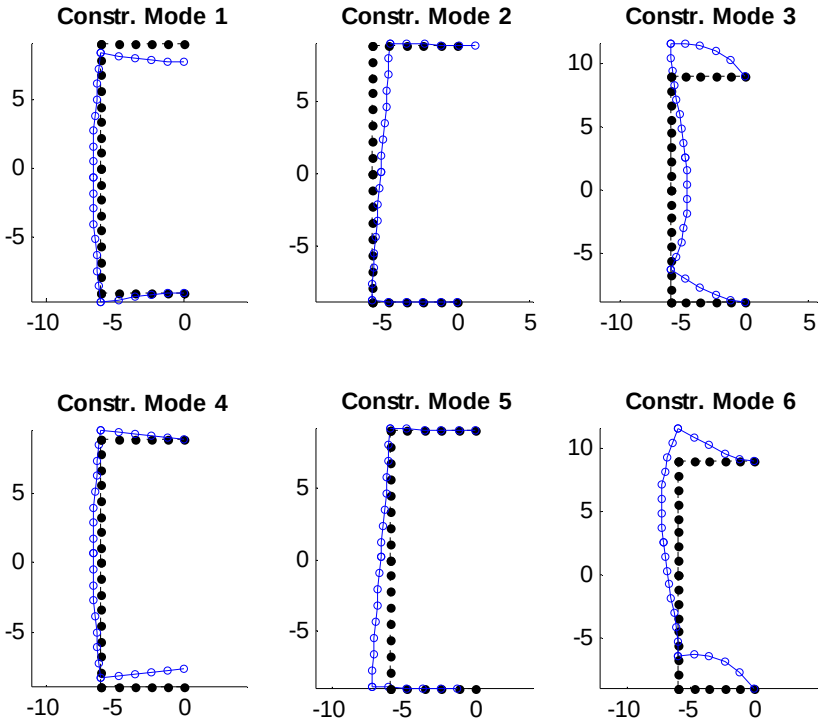

Figure 6: Constraint modes of the transmission simulator.

These "measured" modes for C were combined with the CB model for the transmission simulator and Eq. (9) was used with the constraint in Eq. (10) to compute a model for subcomponent B. In practice the model for B would then be used to predict the response of the assembly of interest, or of various design iterations of that assembly. In this work, the true assembly is already known (via the full finite element model), and so its modes will be compared with those predicted by substructuring to evaluate the CB procedure. Before doing this, two other intermediate cases were considered to seek to explain what information is captured in the "experimentally" derived model for B. First, both of the legs of B were constrained to ground at the connection points. In this case the model for B accurately predicted the first three natural frequencies, with errors of 5% or less, and the next few modes were also quite reasonable with about 10% error. Next, only one leg of B was constrained to ground leaving the other leg free. In this case the model produced qualitatively accurate estimates of the first three modes although their natural frequencies were about 30% too high. This reveals that, while the CB procedure does produce a Craig-Bampton-like model for substructure B, it will not necessarily have the same resolution as a real analytical Craig-Bampton model with the same number of modes. The authors have previously suggested that the best practice is to use a transmission simulator that mimics the interface in the assembly of interest, and the TS used here clearly does this so one would hope that the model for B will be accurate in that assembly.

3.2.1 Results for Assembly of Interest

The true modes of the system in the application of interest are show in Figure 7. Each of the modes estimated by the substructuring procedure was matched to the system modes using the MAC matrix shown in Figure 8. Then, the natural frequencies for the modes that corresponded were compared in Table 3. The substructuring procedure was repeated using the CB-TS method as well as the original FF-TS method from [4]. Both methods used 8 modes to model the transmission simulator. In the case of the FF-TS method, the highest mode was at 2.2 kHz, considerably higher than the highest free-interface mode that the CB-TS model predicted accurately.

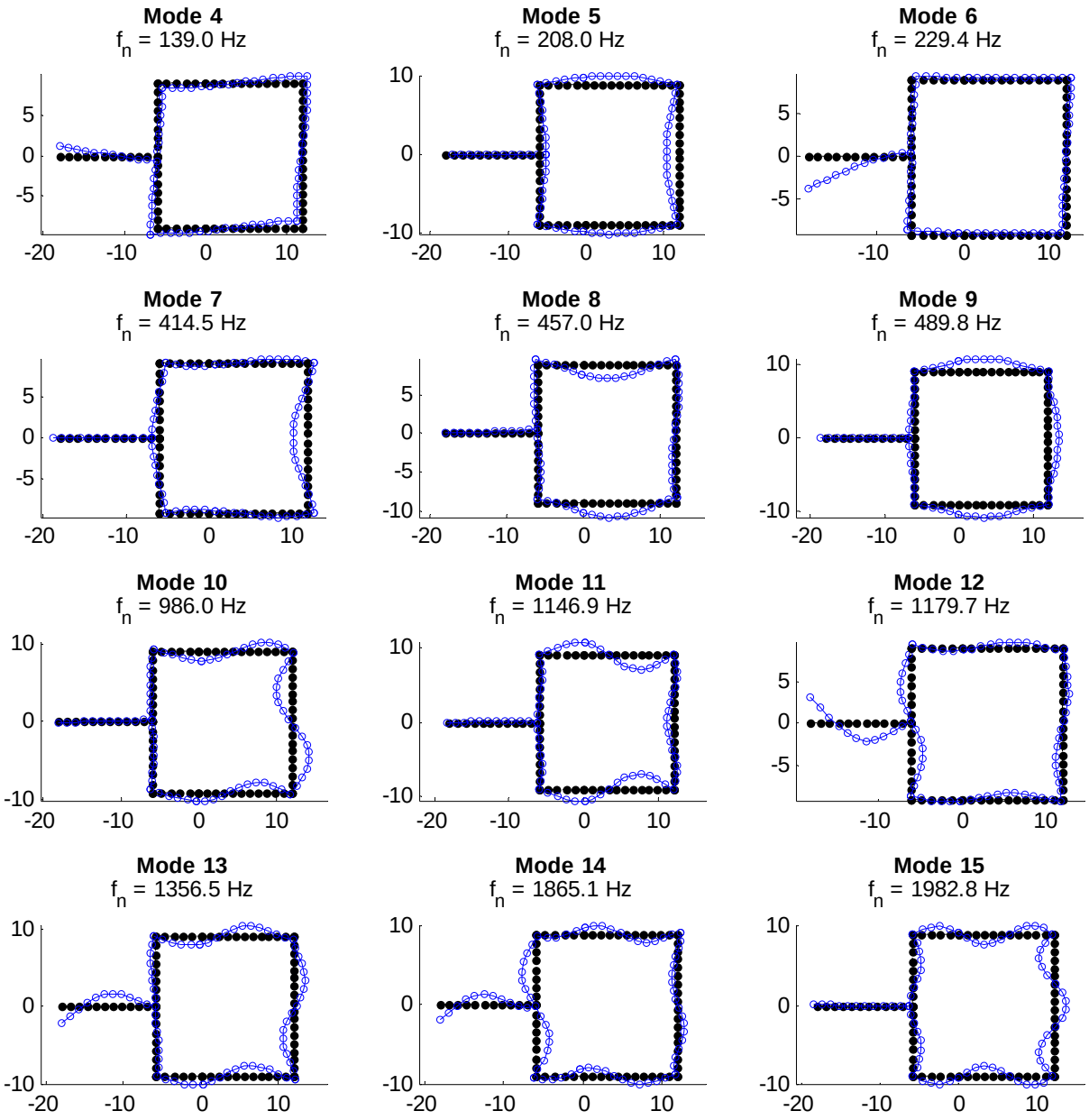

Figure 7: Mode shapes of the truth model for the application of interest.

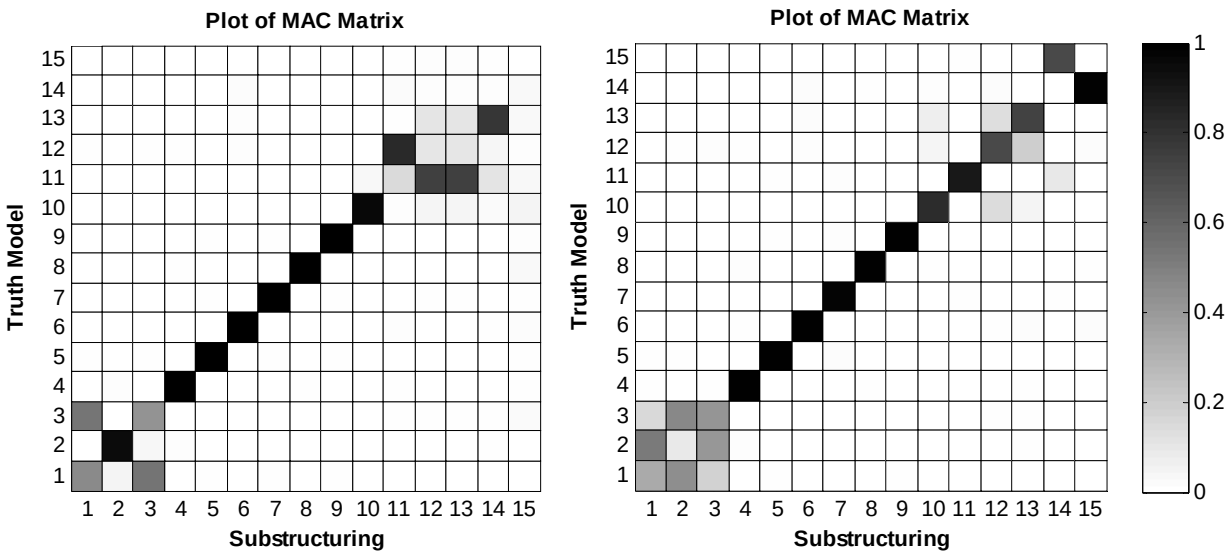

Figure 8: MAC between the Modes of the Truth Model and those predicted by substructuring using the (left) CB-TS and (right) FF-TS methods.

The results in Table 3 show that the CB-TS method produced considerably more accurate estimates for this assembly in the application of interest, at least in the lower frequency range. For the modes below 1kHz (or one third of the frequency range over which the C assembly was tested), the CB method accurately estimated all of the modes with less than 0.5% error in any natural frequency and almost all of the MAC values above 0.999. On the other hand, the FF-TS method also provides reasonable predictions although the frequencies were less accurate, sometimes in error by as much as 16%, and the mode shapes were also somewhat less accurate as shown by the MAC. On the other hand, the FF-TS method provided reasonable estimates of all of the modes below 2kHz while the CB-TS method predicted several spurious modes beginning at 1.2kHz.

Table 3: Natural Frequencies (Hz) of the Assembly of Interest Estimated by Substructuring.

Mode	Truth	N	CB-TS	CB Error	MAC	N	FF-TS	FF-Error	MAC
4	139.0	4	138.8	-0.2%	1.0000	4	128.0	-7.9%	0.9962
5	208.0	5	208.4	0.2%	0.9999	5	200.2	-3.7%	0.9950
6	229.4	6	229.5	0.0%	0.9999	6	228.0	-0.6%	0.9979
7	414.5	7	416.6	0.5%	0.9993	7	396.7	-4.3%	0.9858
8	457.0	8	457.1	0.0%	0.9996	8	452.9	-0.9%	0.9977
9	489.8	9	490.0	0.0%	0.9999	9	488.2	-0.3%	0.9977
10	986.0	10	990.6	0.5%	0.9695	10	887.2	-10.0%	0.8290
11	1146.9	11	1238.0	-		11	962.4	-16.1%	0.9038
12	1179.7	12	1172.0	2.2%	0.8392	12	1134.0	-3.9%	0.7124
13	1356.5	14	1314.3	-3.1%	0.7867	13	1263.4	-6.9%	0.7421
14	1865.1					14	1802.1	-3.4%	0.7132
15	1982.8					15	1854.4	-6.5%	0.9923

These models were found to contain some negative mass, so, as was done in Section 3.1, the "Added Mass" method from [6] was used to add mass to the substructure model for B until its mass matrix became positive definite. Figure 9 and Table 4 show the results when positive mass is forced onto the substructuring results. The ratio of the norm of the mass added to that of the mass matrix in each case was 0.0766 and 0.0226 for the CB-TS and FF-TS methods respectively. While the CB-TS method required three times as much mass to obtain a positive mass matrix, this simple addition of mass improved the results remarkably. With added mass the CB-TS method produced only one spurious mode and predicted all of the modes below 2 kHz quite accurately. On the other hand, the model predicted by the FF-TS method did not improve significantly, except perhaps in its estimates of the rigid body modes.

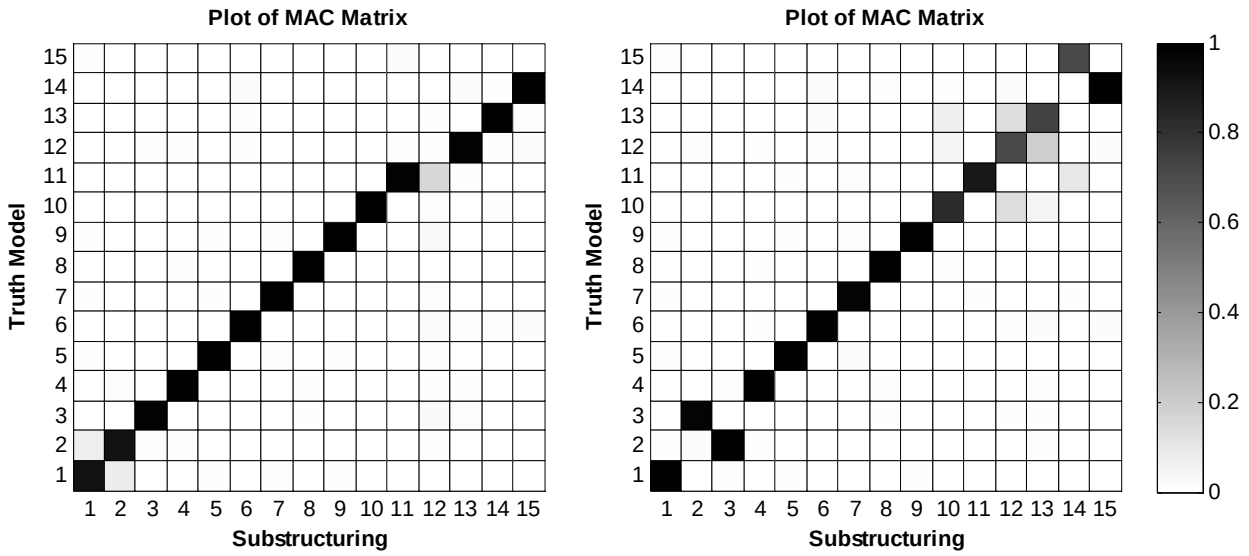

Figure 9: MAC matrices for the cases mentioned in Figure 8, when positive mass is enforced for each method: (left) CB-TS and (right) FF-TS.

Table 4: Natural Frequencies (Hz) of the Assembly of Interest Estimated while enforcing positive mass.

Mode	Truth	N	CB-TS	CB Error	MAC	N	FF-TS	FF-Error	MAC
4	139.0	4	138.3	-0.6%	1.0000	4	128.0	-7.9%	0.9962
5	208.0	5	208.4	0.2%	0.9999	5	200.2	-3.7%	0.9949
6	229.4	6	229.3	-0.1%	0.9999	6	228.0	-0.6%	0.9979
7	414.5	7	415.8	0.3%	0.9997	7	396.7	-4.3%	0.9855
8	457.0	8	456.3	-0.1%	1.0000	8	452.9	-0.9%	0.9977
9	489.8	9	489.7	0.0%	0.9999	9	488.2	-0.3%	0.9974
10	986.0	10	978.8	-0.7%	0.9981	10	887.2	-10.0%	0.8295
11	1146.9	11	1135.3	-1.0%	0.9919	11	962.4	-16.1%	0.9040
12	1179.7	13	1178.3	-0.1%	0.9929	12	1134.0	-3.9%	0.7121
13	1356.5	14	1344.3	-0.9%	0.9967	13	1263.4	-6.9%	0.7416
14	1865.1	15	1866.8	0.1%	0.9981	14	1802.1	-3.4%	0.7152
15	1982.8				-	15	1854.4	-6.5%	0.9949

4. Conclusion

This work has presented an alternative to the Transmission Simulator method in which the TS is modeled with a Craig-Bampton model. This is expected to produce a more accurate model of the TS in applications where the TS is rigidly connected to the subcomponents of interest. The method was validated by applying it to a few simple beam structures and the results showed that this new method did indeed give more accurate estimates of the assembly's natural frequencies. However, if one's goal was to estimate the free modes of the structure of interest (e.g. if it will not be assembled to a rigid component after removing the transmission simulator) then the CB method was somewhat less accurate than the authors' previous approach, which used free-interface modes to model the TS.

The last application presented here explored a potentially ill-conditioned problem of removing a TS that connects to the subcomponent of interest at two points. In this case, one already requires six modes for the constraint modes of the CB model; if the interface was modeled with more points then it would almost certainly be necessary to reduce the interface in some way or there might be more TS modes than there are in system C making this subtraction impossible. In this regard, the traditional FF-TS method is convenient as it simply uses the free modes of the transmission simulator to approximate the interface so this does not become an issue unless the system is such that too many free modes are required to adequately model the TS.

Acknowledgements

This work was supported by Sandia National Laboratories. Notice: This manuscript has been authored by Sandia Corporation under Contract No. DE-AC04-94AL85000 with the U.S. Department of Energy. The United States Government retains and the publisher, by accepting the article for publication, acknowledges that the United States Government retains a non-exclusive, paid-up, irrevocable, world-wide license to publish or reproduce the published form of this manuscript, or allow others to do so, for United States Government purposes.

References

[1] D. de Klerk, D. J. Rixen, and S. N. Voormeeren, "General framework for dynamic substructuring: History, review, and classification of techniques," *AIAA Journal*, vol. 46, pp. 1169-1181, 2008.

[2] M. S. Allen and R. L. Mayes, "Comparison of FRF and Modal Methods for Combining Experimental and Analytical Substructures," presented at the 25th International Modal Analysis Conference (IMAC XXV), Orlando, Florida, 2007.

[3] R. L. Mayes and E. C. Stasiunas, "Lightly Damped Experimental Substructures for Combining with Analytical Substructures," presented at the 25th International Modal Analysis Conference (IMAC XXV), Orlando, Florida, 2007.

[4] M. S. Allen, R. L. Mayes, and E. J. Bergman, "Experimental Modal Substructuring to Couple and Uncouple Substructures with Flexible Fixtures and Multi-point Connections," *Journal of Sound and Vibration*, vol. 329, pp. 4891–4906, 2010.

[5] M. S. Allen, D. C. Kammer, and R. L. Mayes, "Metrics for Diagnosing Negative Mass and Stiffness when Uncoupling Experimental and Analytical Substructures," *Journal of Sound and Vibration*, vol. 331, pp. 5435–5448, 2012.

[6] R. L. Mayes, M. S. Allen, and D. C. Kammer, "Correcting indefinite mass matrices due to substructure uncoupling," *Journal of Sound and Vibration*, vol. 332, pp. 5856-5866, 2013.

[7] R. L. Mayes and M. Arviso, "Design Studies for the Transmission Simulator Method of Experimental Dynamic Substructuring," presented at the International Seminar on Modal Analysis (ISMA2010), Lueven, Belgium, 2010.

[8] R. L. Mayes and M. R. Ross, "Advancements in hybrid dynamic models combining experimental and finite element substructures," *Mechanical Systems and Signal Processing*, vol. 31, pp. 56-66, 2012.

[9] R. R. Craig and M. C. C. Bampton, "Coupling of Substructures for Dynamic Analysis," *AIAA Journal*, vol. 6, pp. 1313-1319, 1968.

[10] D. C. Kammer, M. S. Allen, and R. L. Mayes, "Formulation of a Craig-Bampton Experimental Substructure Using a Transmission Simulator," presented at the 31st International Modal Analysis Conference (IMAC XXXI), Garden Grove, CA, 2013.

[11] R. R. J. Craig, *Structural Dynamics*. New York: John Wiley and Sons, 1981.

[12] P. Ind, "The Non-Intrusive Modal Testing of Delicate and Critical Structures," PhD Ph.D., Imperial College of Science, Technology & Medicine, University of London, London, 2004.